



ELSEVIER

Journal of Nuclear Materials 283–287 (2000) 147–151

Journal of  
nuclear  
materials

www.elsevier.nl/locate/jnucmat

Section 2. Fundamentals of radiation effects

# Radiation-induced inter-granular segregation in first wall fusion reactor materials

R.G. Faulkner<sup>a,\*</sup>, S. Song<sup>a</sup>, P.E.J. Flewitt<sup>b</sup>

<sup>a</sup> *Institute of Polymer Technology and Materials Engineering (IPTME), Loughborough University, Loughborough, Leics, LE11 3TU, UK*

<sup>b</sup> *BNFL Magnox Generation, Berkeley Technical Centre, Berkeley, Glos, GL13 9PB, UK*

## Abstract

Experimental evidence for phosphorus segregation at grain boundaries in steels is presented. Theories for irradiation-induced inter-granular segregation are described. Non-equilibrium segregation (NES) and rate theory approaches have similar success in predicting phosphorus behaviour in the practically important temperature range although site competition and micro-structural effects are better accounted for by the NES theory. The need for better data on diffusion constants and point defect-impurity binding energy is emphasised. © 2000 Elsevier Science B.V. All rights reserved.

## 1. Introduction

This paper will concentrate on the inter-granular segregation behaviour of phosphorus in pressure vessel steels. This topic is of interest to the fusion community because of the possible use of ferritic–martensitic steels for first wall applications. These steels are similar to the pressure vessel low alloy steels discussed here. The behaviour of phosphorus at grain and lath boundaries during irradiation has consequences for mechanical properties in all ferritic steels and it is therefore thought that a review of modelling of and experimental data relating to this phenomenon is relevant to fusion reactor materials development.

The paper will be divided into two main sections: experimental and theoretical. Because of the difficulty in carrying out long term test irradiations, and the increasing lack of availability of neutron sources for this purpose, the data considered here are taken from the literature based upon dedicated experimental reactor surveillance schemes. These are less complete than is ideal for comparison with the theoretical predictions.

Apart from the early fundamental studies by Johnson and Lam [1] on Ag–Zn, most of the practical studies have centered on the behaviour of phosphorus in ferritic steels and on chromium in austenitic steels. Theory has been based on two main approaches: non-equilibrium or solute drag mechanisms and rate theory or inverse Kirkendall effect mechanisms. Notable success of the various models depends upon the availability of suitable data on binding energies, site competition parameters, and diffusion data, much of which is likely to be supplied in future by molecular dynamics calculations.

## 2. Experimental observation of radiation-induced grain boundary segregation

The techniques used for the analytical determinations are a mixture of field emission gun transmission electron microscope (FEGTEM) and Auger electron spectroscopy (AES) results [3,4,10,14,15]. The AES results are likely to be biased because they are obtained from the weakest boundaries and thus heavily emphasise the element responsible for initiating inter-granular failure. The FEGTEM results are likely to be underestimates because beam spreading produces a signal from a slightly wider region than one monolayer. There are many conversions of fractional monolayer coverage to

\* Corresponding author. Tel.: +44-1509 223 153; fax: +44-1509 223 949.

E-mail address: r.g.faulkner@lboro.ac.uk (R.G. Faulkner).

atomic percent measured on the grain boundary. The method used here is to assume that 100% monolayer coverage is equivalent to 25 at.% concentration. This is based on the assumption that the grain boundary is approximately four close packed planes in width. Enrichment factors are then determined using a knowledge of the bulk impurity element content in the alloy.

We here consider phosphorus grain boundary segregation in C–Mn and low alloy ferritic pressure vessel steels [3,4,10,14,15]. These will have a range of microstructures but the grain boundaries investigated will be a mixture of lath ferrite or prior austenite type. A survey of the experimental results obtained for P grain boundary segregation as a function of temperature for a variety of pressure vessel steels is shown in Fig. 1 (reference key used in Fig. 1 is provided in Table 1). It should be emphasised that these results come from experiments with widely-differing conditions of dose, dose rate, composition and microstructure and should therefore only be reviewed in a qualitative sense. The enrichment caused by equilibrium and non-equilibrium processes occurring during prior heat treatment (solution treatment, ageing, welding, and stress relief annealing) was subtracted from the results shown in Fig. 1.

Several general observations about phosphorus segregation behaviour in steels can be made. The first is that segregation, as shown in Fig. 1, gradually increases with temperature. A least squares fitting line supports this conclusion. Modelling work on the temperature dependence of segregation [3] suggests that there are two peaks; one at lower temperature (150–300°C), is believed to be due to non-equilibrium segregation, caused by streams of point defect-impurity complexes produced by neutron irradiation arriving at the boundaries. The

second higher temperature peak (>350°C) is due to thermal equilibrium segregation. Secondly, there is evidence of site competition effects, particularly from carbon. The effect of increasing carbon causing reduced phosphorus segregation is reported in the work of Beere [2], and solute drag models substantially over-predict the enrichment shown in Fig. 1 if site competition is not included [3]. Kameda and Bevolo [4] have also reported a reduction in phosphorus segregation with increasing carbon content. Thirdly, increasing irradiation dose increases the amount of phosphorus segregation, but there does seem to be a saturation limit [3,10].

There have been studies of segregation at even higher resolution than FEGTEM or AES. Atom probe field ion

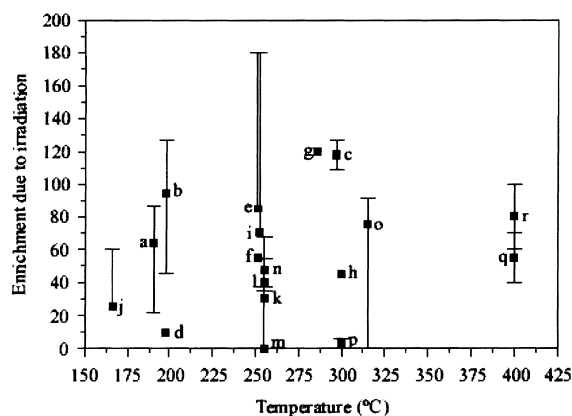


Fig. 1. Temperature dependence of measured inter-granular phosphorus enrichment after irradiation at dose rates between  $10^{-9}$  and  $10^{-12}$  dpa  $s^{-1}$  and for doses up to 30 mdpa.

Table 1  
Reference key for Fig. 1

Key	Reference	Dose (mdpa)	Dose rate (dpa $s^{-1}$ )	Technique
a	Jones et al. [16]	2.656	$3 \times 10^{-12}$	AES
b	Jones et al. [16]	1.5	$3.7 \times 10^{-12}$	AES
c	Jones et al. [16]	1.93	$3 \times 10^{-12}$	AES
d	Druce et al. [10]	0.94	$1 \times 10^{-12}$	FEGTEM
e	Druce et al. [10]	9.3	$1 \times 10^{-9}$	FEGTEM
f	Druce et al. [10]	9.2	$1 \times 10^{-9}$	AES
g	Druce et al. [10]	9.5	$1 \times 10^{-9}$	AES
h	Druce et al. [10]	1.52	$1 \times 10^{-12}$	FEGTEM
i	Druce et al. [10]	8.61	$1 \times 10^{-9}$	FEGTEM
j	Druce et al. [10]	9.11	$1 \times 10^{-9}$	FEGTEM
k	Meade [15]	1.5	$8.9 \times 10^{-11}$	FEGTEM
l	Meade [15]	12.3	$6.4 \times 10^{-10}$	FEGTEM
m	Meade [15]	29.0	$6 \times 10^{-9}$	FEGTEM
n	Meade [15]	38.0	$6 \times 10^{-9}$	FEGTEM
o	Meade [15]	26.6	$6.3 \times 10^{-9}$	FEGTEM
p	Faulkner et al. [3]	42	$1.05 \times 10^{-8}$	FEGTEM
q	Faulkner et al. [3]	130	$1.75 \times 10^{-8}$	FEGTEM
r	Kameda and Bevolo [4]	6.6	$1.5 \times 10^{-8}$	AES

microscopy (APFIM) has confirmed the presence of P and Mo on grain boundaries in VVER pressure vessel steels [5].

### 3. Modelling of radiation-induced inter-granular segregation

Two modelling approaches have been adopted. The first is to model non-equilibrium segregation (NES) or solute drag effects [3]: this represents a simplified method, which has the advantages that fewer data are required to fit parameters, site competition effects can be included, and microstructural effects are easier to incorporate. The model assumes that excess non-equilibrium point defects are formed during non-equilibrium processes such as quenching and neutron irradiation and that these become absorbed at a sink, like a grain boundary. This sets up a point defect concentration gradient around the sink, which can be quantified in terms of the non-equilibrium process producing it. If impurity atoms in the material have a positive binding energy with the point defects, then some of these impurities will be dragged towards the boundary down the point defect concentration gradient. If the diffusion constants of these complexes can be estimated, then the kinetics and magnitude of the impurity enrichment can be predicted. During irradiation it is assumed that the self-interstitials are the dominant point defect for NES, because they have the highest binding energies with typical impurities and because they have very low activation energies for diffusion [3]. As a consequence the key equations used to predict the magnitude and kinetics of the segregation, taking into account site competition, have been derived in a previous study [3], and are as follows.

$$C_{\text{br}(Sj)}^m = C_g^{Sj} \frac{E_{\text{b}(Sj)}^{\text{ip}}}{E_{\text{f}}^{\text{p}}} \left[ \frac{C_g^{Sj} \exp(E_{\text{b}(Sj)}^{\text{ip}}/kT)}{\sum_j C_g^{Sj} \exp(E_{\text{b}(Sj)}^{\text{ip}}/kT)} \right] \times \left[ 1 + \frac{BGF(\eta)}{A_p D_p k_{\text{dp}}^2} \exp\left(\frac{E_{\text{f}}^{\text{p}}}{kT}\right) \right] \quad (j = 1, 2) \quad (1)$$

and

$$\frac{C_{\text{br}(Sj)}^{Sj}(t) - C_g^{Sj}}{C_{\text{br}(Sj)}^m - C_g^{Sj}} = 1 - \exp\left(\frac{4D_{\text{c}(Sj)}^{\text{ip}} t}{\alpha_{\text{n}(Sj)}^2 d^2}\right) \times \text{erfc}\left(\frac{2\sqrt{D_{\text{c}(Sj)}^{\text{ip}} t}}{\alpha_{\text{n}(Sj)} d}\right) \quad (j = 1, 2), \quad (2)$$

where  $C_{\text{br}(Sj)}^m$  is the maximum time-independent concentration of the  $Sj$ th element on the boundary;  $C_g^{Sj}$  the grain concentration of the  $Sj$ th element;  $E_{\text{b}(Sj)}^{\text{ip}}$  the in-

terstitial-impurity ( $Sj$ ) binding energy;  $E_{\text{f}}^{\text{p}}$  the interstitial formation energy;  $k$  is Boltzmann's constant;  $T$  the absolute temperature;  $B$  the proportion of freely migrating defects (assumed to be 1%);  $G$  the point defect generation rate.  $F(\eta)$  is the recombination rate, discussed more fully in [3];  $A_p$  the pre-exponential term in the equation describing the interstitial concentration;  $D_p$  the interstitial diffusion coefficient;  $k_{\text{dp}}^2$  the sink efficiency of the matrix for the interstitial point defect, taking into account the dislocation density and grain size;  $C_{\text{br}(Sj)}^{Sj}(t)$  the boundary concentration of the  $Sj$ th element after time  $t$ ;  $D_{\text{c}(Sj)}^{\text{ip}}$  the complex diffusion coefficient for the  $Sj$ th element;  $\alpha_{\text{n}(Sj)}$  the maximum enrichment ratio for the  $Sj$ th element, i.e.,  $C_{\text{br}(Sj)}^m/C_g^{Sj}$ ; and  $d$  is the grain boundary width (assumed to be 1 nm). All the diffusion coefficients are irradiation enhanced, using methods described in [3]. Site competition is totally accounted for by assuming that  $C_{\text{br}(Sj)}^{Sj}(t)$  is modified to  $C_{\text{br}(Sj)}^{Sj}(t)^*$ , according to the relative binding energies between the segregated species and the grain boundary,  $Q_{Sj}$ .

$$C_{\text{br}(Sj)}^{Sj}(t)^* = C_{\text{br}(Sj)}^{Sj}(t) \left( \frac{C_g^{S1} \exp(Q_{S1}/kT)}{C_g^{S1} \exp(Q_{S1}/kT) + C_g^{S2} \exp(Q_{S2}/kT)} \right), \quad (3)$$

where (2) represents the competitive species. The NES model further indicates that after a critical time saturation will take place and a permanent segregation situation will continue until the radiation conditions are changed.

The second modelling approach is the more rigorous rate theory, or inverse Kirkendall model [1,6–9]. A series of partial second-order differential equations is set up to describe the time dependence of the concentrations of point defects and all elements present as a function of irradiation conditions and time. These equations are solved simultaneously to forecast the behaviour, particularly of the impurity species, in the neighbourhood of grain boundaries. Many of the data required are not currently available, and so curve fitting to the available experimental data is employed. The results of Druce et al. [10] presented below are based on this model and are fitted to data on phosphorus segregation in ferritic steel by varying the self interstitial-phosphorus binding energy.

### 4. Model parameters

The most inscrutable parameters required for modelling are those connected with the diffusion characteristics of the self-interstitial-impurity complexes and the impurity-self-interstitial binding energy. The complex diffusion can take place in bcc lattices by a variety of mechanisms. Barbu and Lidiard [11] have treated these,

and it seems that the most likely mechanism is the  $\langle 110 \rangle$  split dumbbell rotation to  $\langle 111 \rangle$  followed by interstitial crowdion migration along  $\langle 111 \rangle$ . Under these circumstances we have assumed that the total energy required to move the complex involves dissociating a self-interstitial/impurity atom complex (energy required is the binding energy for this complex,  $E_{ip}^b$ ), followed by migration of the interstitial (energy required,  $E_m^p$ ) [16]. The activation energy for diffusion of the complex (diffusion coefficient  $D_{c(Sj)}^{ip}$ ) is taken as the sum of the two above energies.

The interstitial binding energy is derived from a continuum elasticity analysis of the lattice surrounding the impurity atom in the interstitial-impurity split  $\{110\}$  dumbbell configuration [17]. Although Hardy and Bulough [12] have shown that lattice statics based on the discrete nature of the lattice is a better approach to use, we feel justified in using continuum elasticity because the continuum approach only breaks down when interactions out at several lattice spacings are considered. We are considering nearest neighbour interactions primarily in this instance. The continuum approach on an atomic scale seems a good approximation for metals since there are no strong anisotropic constraints with electronic bonding in metals as there are for non-metallic bonding within ceramics or polymers. It may be that in the future molecular dynamics calculations will provide answers to these binding energy questions (e.g., [13]).

Fig. 2 shows the theoretical predictions from the solute drag model of phosphorus inter-granular segregation in ferritic steels as a function of temperature (dislocation density,  $1 \times 10^{-15} \text{ m}^{-2}$ , grain size  $10 \mu\text{m}$ , dose rate  $5 \times 10^{-12} \text{ dpa s}^{-1}$ , dose 5 mdpa). Two free carbon contents are included in the solute drag theory

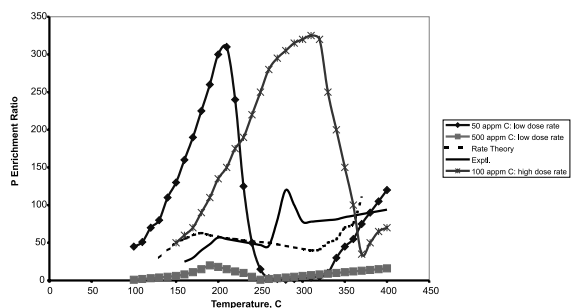


Fig. 2. Theoretical predictions of phosphorus inter-granular segregation in ferritic steels as a function of temperature (dislocation density,  $1 \times 10^{-15} \text{ m}^{-2}$ , grain size  $10 \mu\text{m}$ , dose rate  $5 \times 10^{-12} \text{ dpa s}^{-1}$ , dose 5 mdpa). A summary of the experimental data from Fig. 1 is also included. Two carbon contents are included in the solute drag theory predictions. Another solute drag prediction for a higher dose rate and dose ( $1 \times 10^{-8} \text{ dpa s}^{-1}$  and 130 mdpa) is included. The rate theory predictions are taken from Druce et al. [10].

predictions (50 and 500 appm). Another solute drag prediction for a higher dose rate and dose ( $1.75 \times 10^{-8} \text{ dpa s}^{-1}$  and 130 mdpa) and an intermediate free carbon content (100 appm) is also included. The rate theory predictions are taken from Druce et al. [10]. A summary of the experimental data from Fig. 1 is also included. These experimental data are averaged where data points are clustered at a single temperature (200°C, 260°C, 280°C and 300°C) and points  $p$  and  $q$  are omitted because they are from a 2.25%Cr 1Mo steel, not a C–Mn pressure vessel material. The model parameters used are identical to those quoted for phosphorus segregation in steels in [3].

## 5. Discussion

The important modelling issue is that the solute drag–NES model is very sensitive to the site competition effect when carbon is considered (Fig. 2). The free carbon competes for sites on the grain boundary and within the complexes that are transporting the phosphorus to the grain boundary. The rate theory predictions of Druce et al. [10] give quite good fits with observed data, because they have been curve fitted. This implicitly accounts for any site competition for the alloy concerned. Predicted curves are shown in Fig. 2 for the solute drag model for two carbon concentrations at the lower dose rate ( $5 \times 10^{-12} \text{ dpa s}^{-1}$ ). The carbon concentrations represent the free carbon content, after the carbon required for the carbides has been subtracted from the alloy composition. An independent metallographic study on a 0.4 at.% C–0.14 at.% P–2.25%Cr–1.0%Mo steel has shown that the free carbon content is around 0.11 at.% (1100 appm) with a slightly lower stress relieving temperature (400°C) than typical for pressure vessel steels (650°C). This indicates that a good estimate of the free carbon content for the steels in Fig. 2 is somewhere below 500 appm. Furthermore since the experimental data lie between the 50 and 500 appm free carbon curves at temperatures less than 250°C, this would suggest that the free carbon content of the steels lies somewhere between these two values.

The small peak seen in the experimental curve at about 290°C can be seen to coincide with the solute drag model predictions in position but not magnitude for the high dose rate ( $1.75 \times 10^{-8} \text{ dpa s}^{-1}$ ; 130 mdpa). The magnitude of the peak in this high dose rate curve is much higher than that suggested by the experimental values. This is because this curve was approximately appropriate in terms of free carbon levels and dose rate for many of the experimental data, but the dose was very high (130 mdpa; compared to the majority of the experimental data which are from doses of up to 10 mdpa).

It is worth commenting further that the experimental techniques used to give the experimental curve differed. As mentioned earlier, where Auger electron spectroscopy (AES) is used the enrichment ratio is artificially high because the intergranular fracture necessary for these measurements always occurs along the most heavily segregated boundaries.

Another comment is that we show elsewhere [18] that irradiation and higher temperatures (up to 400°C) shift the DBTT upwards in 2.25Cr 1Mo steels. This correlates well with the P intergranular segregation behaviour described here, although matrix hardening effects must clearly also be considered in the assessment.

## 6. Conclusions

A summary of existing experimental results for phosphorus grain boundary segregation in ferritic pressure vessel steels has been presented. The data show that phosphorus segregation is enhanced by neutron irradiation. The temperature dependence of the irradiation induced segregation is complex but is now reasonably well understood. In the 150–300°C temperature regime NES mechanisms are important. At temperatures above about 350°C thermal equilibrium segregation dominates. Site competition arguments and available experimental data suggest that elements like carbon play a major role in controlling phosphorus segregation. Model predictions of the temperature dependence of non-equilibrium segregation based on (a) non-equilibrium solute drag theory and (b) rate theory or Inverse Kirkendall theory support the data, although site competition and microstructural effects are currently more completely described by the solute drag theory. Better data on complex diffusion coefficients and impurity-point defect binding energies are needed.

## Acknowledgements

The authors wish to thank BNFL Magnox Generation for funding this work.

## References

- [1] R.A. Johnson, N.Q. Lam, *Phys. Rev.* 13 (1976) 4364.
- [2] W.B. Beere, BNFL Magnox Generation, 1988, private communication.
- [3] R.G. Faulkner, S. Song, P.E.J. Flewitt, M. Victoria, P. Marmy, *J. Nucl. Mater.* 255 (1998) 189.
- [4] J. Kameda, A.J. Bevolo, *Acta. Metall.* 37 (1989) 3283.
- [5] M.K. Miller, M.G. Burke, 195 (1992) 68.
- [6] P.R. Okamoto, H. Wiedersich, *J. Nucl. Mater.* 53 (1974) 336.
- [7] Y. Grandjean, P. Bellon, G. Martin, *Phys. Rev. B* 50 (1994) 4228.
- [8] E.P. Simonen, E.R. Bradley, R.H. Jones, in: N.H. Packan et al. (Eds.), *Effects of Irradiation on Materials*, ASTM STP 1046, 1989, p. 411.
- [9] T. Hashimoto, *Proceedings of the Symposium on Diffusion in Materials*, CARET, Hokkaido University, 1997.
- [10] S.G. Druce, C.A. English, A.J.E. Foreman, R.J. McElroy, I.A. Vatter, C.J. Bolton, J.T. Buswell, R.B. Jones, in: D.S. Gelles, R.K. Nanstead, A.S. Kumar, E.A. Little (Eds.), *Proceedings of the 17th Symposium on Radiation Effects in Materials*, ASTM STP 1270, Philadelphia, 1996, p. 119.
- [11] A. Barbu, A.B. Lidiard, *Philos. Mag. A* 74 (1996) 709.
- [12] J.R. Hardy, R. Bullough, *Philos. Mag.* 15 (1967) 237.
- [13] A.F. Calder, D.J. Bacon, *J. Nucl. Mater.* 207 (1993) 25.
- [14] D. Meade, 1998, PhD thesis, Loughborough University, p. 238.
- [15] R.B. Jones, J.R. Cowan, R.C. Corcoran, J.C. Walmsley, BNFL-Magnox Generation, 1998, private communication.
- [16] R.G. Faulkner, S. Song, C.C. Goodwin, P.E.J. Flewitt, *Def. Diffus. Forum* 165&166 (1999) 29.
- [17] R.G. Faulkner, S. Song, P.E.J. Flewitt, *Mater. Sci. Technol.* 12 (1996) 904.
- [18] S. Song, R.G. Faulkner, P.E.J. Flewitt, R.F. Smith, P. Marmy, M. Victoria, *J. Nucl. Mater.* 280 (2000) 162.